

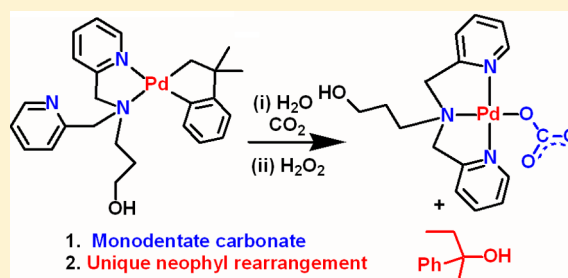
Reactivity of a Palladacyclic Complex: A Monodentate Carbonate Complex and the Remarkable Selectivity and Mechanism of a Neophyl Rearrangement

Ava Behnia, Mahmood A. Fard, Johanna M. Blacquiere,* and Richard J. Puddephatt*[†]

Department of Chemistry, University of Western Ontario, London, Ontario N6A 5B7, Canada

Supporting Information

ABSTRACT: The ligand $N(\text{CH}_2\text{-}2\text{-C}_5\text{H}_4\text{N})_2(\text{CH}_2\text{CH}_2\text{CH}_2\text{OH})$, **L1**, reacted with $[\text{Pd}(\text{CH}_2\text{CMe}_2\text{C}_6\text{H}_4)(\text{COD})]$ to give a new fluxional “cycloneophyl” organopalladium complex $[\text{Pd}(\text{CH}_2\text{CMe}_2\text{C}_6\text{H}_4)(\kappa^2\text{-L1})]$, **1**, which on attempted recrystallization from THF gave the monodentate carbonate complex $[\text{Pd}(\text{CO}_3)(\kappa^3\text{-L1})]$, **2**. Complex **2** was prepared in designed syntheses by reaction of $[\text{PdCl}(\kappa^3\text{-L1})]^+$ with silver carbonate or by reaction of $[\text{Pd}(\text{OH})(\kappa^3\text{-L1})]^+$ with CO_2 . Complex **1** reacted with aqueous CO_2 to give the cationic neophylpalladium complex $[\text{Pd}(\text{CH}_2\text{CMe}_2\text{C}_6\text{H}_5)(\kappa^3\text{-L1})]^+(\text{HCO}_3)^-$, **6**. Complex **6** reacts with hydrogen peroxide to give complex **2** with release of a mixture of organic products, the major one being 2-phenyl-2-butanol, **PB**. The formation of **PB** involves a neophyl rearrangement with the unprecedented preference for methyl over phenyl migration. A mechanistic basis for this unexpected reaction is proposed, involving β -carbon elimination at a palladium(IV) center.



INTRODUCTION

Catalytic oxidation of organic compounds using plentiful and environmentally benign oxidants, such as H_2O_2 and O_2 , is highly desirable.¹ A major ongoing challenge in this field is to improve oxidation selectivity and this is driving many fundamental studies into the reactivity and mechanism of key oxidation steps.^{1,2} Specifically, organopalladium(II) complexes with hard nitrogen-donor ligands oxidize with H_2O_2 to give reactive palladium(IV) intermediates that can undergo reductive elimination with C–O bond formation.² For example, complex **A**, with the bulky $\text{MesN}=\text{CC}=\text{NMes}$ (Mes = mesityl) ligand, reacts with hydrogen peroxide to give the product of oxygen atom insertion, **B**, probably by an oxidative addition–reductive elimination sequence, whereas complex **C**, with a potentially tridentate triazacyclononane ligand, gives stable palladium(IV) complex **D** (Scheme 1).² In related organoplatinum chemistry, ligands with pendent hydroxyl groups enhance reactivity toward oxidation by H_2O_2 or O_2 . Thus, dimethylplatinum(II) complexes **E** and **G** are oxidized by hydrogen peroxide and dioxygen, respectively, to give **F** and **H** (Scheme 1).³ The proton-coupled electron transfer reactions, which are possible with ligands of the type shown in Scheme 1, have general significance in several areas of chemistry.⁴

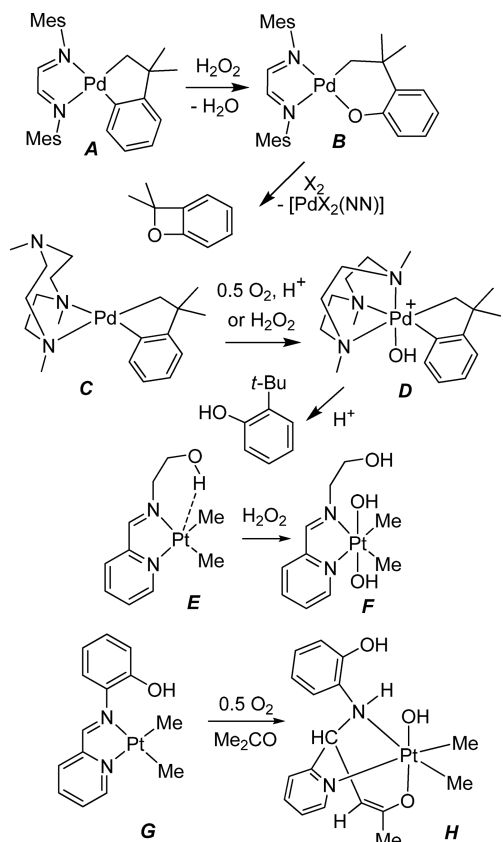
The “cycloneophyl”, $\text{CH}_2\text{CMe}_2\text{C}_6\text{H}_4$, group (**A–D**, Scheme 1) has proven to be particularly valuable in studies of reactivity and selectivity in organopalladium chemistry.^{2,5,6} The group is ideally suited to assess selectivity as it contains both Pd–Csp^3 and Pd–Csp^2 bonds, and the $\text{C}(\text{Me})_2$ group prevents any complicating β -hydride elimination pathways. In order to further increase the reactivity of palladium(II) complexes

toward oxidation by dioxygen or hydrogen peroxide, we have studied the cycloneophylpalladium(II) complex with the ligand $\text{HO}(\text{CH}_2)_3\text{N}(\text{CH}_2\text{-}2\text{-py})_2$, **L1**, py = pyridyl.⁷ The ligand is expected to bind to give $[\text{Pd}(\text{CH}_2\text{CMe}_2\text{C}_6\text{H}_4)(\kappa^2\text{-L1})]$, **1**, in which **L1** binds through the amine and one pyridyl group, leaving one free pyridyl group to act in an analogous way as the free nitrogen donor in **C** and a free hydroxyl group to act in an analogous way as those in **E** and **G** (Scheme 1). Efforts to isolate palladium(IV) complexes are ongoing, but this paper reports two unexpected and interesting observations. The first is that complex **1** can fix carbon dioxide from the air to give the first example of a monodentate carbonate complex of palladium(II), $[\text{Pd}(\kappa^1\text{-CO}_3)(\kappa^3\text{-N,N',N''-L1})]$, and the second is that the reaction involves a unique type of the “neophyl rearrangement”. Some background information to place these observations in context is given below.

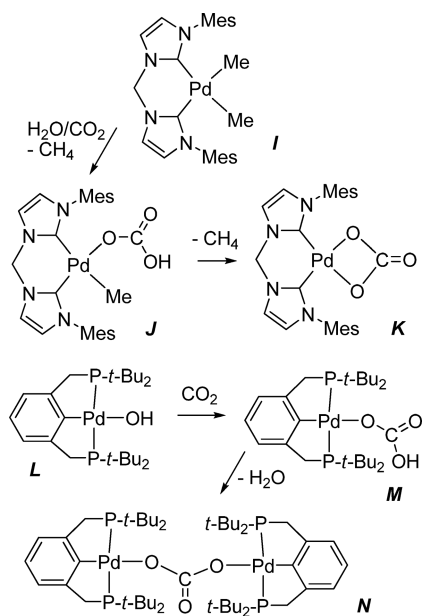
The fixation of CO_2 from the air and conversion to useful organic products are considerable challenges and the subjects of much current research.⁸ One approach is to trap CO_2 by complexes of catalytically active metals, often to give carbonate or carboxylate derivatives, followed by conversion to organic derivatives. In this context, several carbonate and bicarbonate complexes of palladium(II) are known, and they can often be prepared by reactions involving $\text{CO}_2/\text{H}_2\text{O}$ or carbonic acid.^{9–11} For example, **J** (Scheme 2) can be prepared from corresponding dimethylpalladium(II) complex, **I**, by protonolysis with $\text{CO}_2/\text{H}_2\text{O}$ and can then undergo further loss of

Received: August 18, 2017

Scheme 1. Diverse Oxidation Reactivity Achieved with Simple Diimine Ligand (A, B), Ligand with Pendent Nitrogen Donor Group (C, D), and Ligands with Pendent Alcohol or Phenol Group (E–H)



Scheme 2. Some Known Carbonate and Bicarbonate Complexes of Palladium(II)

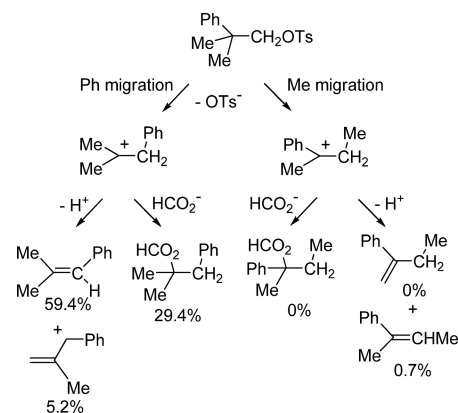


methane to give bidentate carbonate complex **K**.⁹ Hydroxopalladium(II) complex **L** reacts with CO₂ to give monodentate bicarbonate complex **M**, which can eliminate water to give binuclear bridging carbonate complex **N**.¹⁰

However, to the best of our knowledge, no monodentate carbonate complexes of palladium have been reported.

The neophyl rearrangement can be observed in reactions involving either free radical or carbocation intermediates. In free radical reactions, there is often a competition between hydrogen abstraction by the primary radical PhCMe₂CH₂• to give *t*-butylbenzene or rearrangement by phenyl group migration to give PhCH₂CMe₂•, followed by disproportionation or dimerization of this rearranged radical.^{12,13} No products that would arise from the radical MeCH₂CMePh•, which would be formed by methyl group migration in the primary neophyl radical, were observed in this or subsequent studies.^{12,13} Similarly, in neophyl cations or incipient cations formed in solvolysis reactions, phenyl migration always occurs to a greater extent than does methyl migration.¹⁴ For example, formolysis of neophyl tosylate occurred only 0.7% by methyl migration (Scheme 3).^{14b} Mechanisms involving radical or cationic intermediates can be distinguished by the characteristic product mixtures formed.^{12–14}

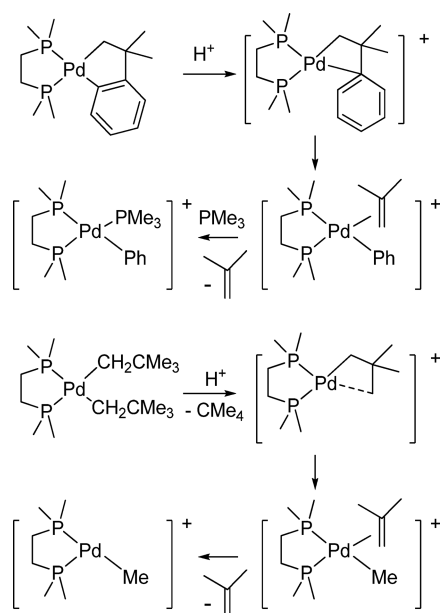
Scheme 3. Neophyl Carbocation Rearrangement



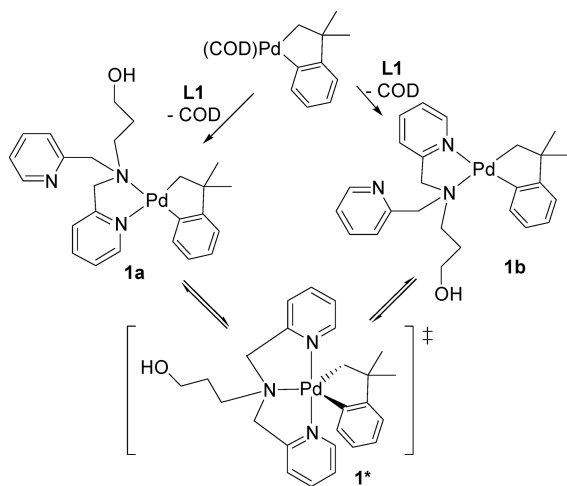
Selective phenyl migration also occurs in the β -carbon elimination from a cationic neophylpalladium(II) complex,¹⁵ though methyl migration can occur in neopentyl complexes, as determined by mass spectrometry (Scheme 4).^{16,17} In contrast to all of the above examples, the reactions reported in this paper give organic products that are formed mostly by methyl migration in the neophyl rearrangement, and the mechanistic basis for this unique selectivity will be discussed.

RESULTS AND DISCUSSION

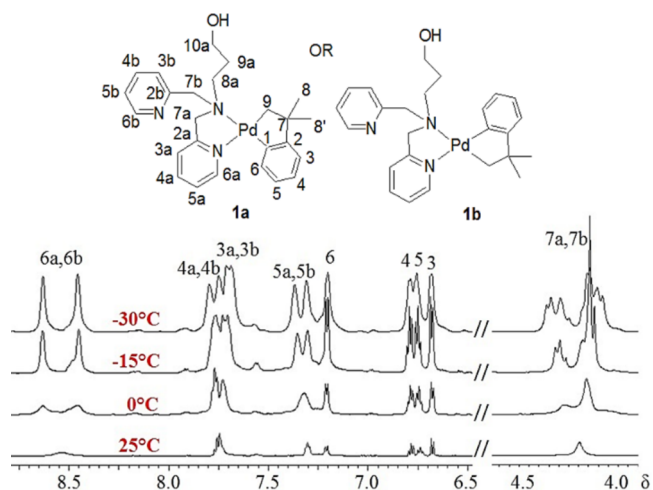
The complex [Pd(CH₂CMe₂C₆H₄)(κ^2 -N,N'-L1)], **1**, was prepared by ligand exchange from the corresponding 1,5-cyclooctadiene complex [Pd(CH₂CMe₂C₆H₄)(COD)]^{2,5,6} and the known ligand *N,N*-bis(pyrid-2-ylmethyl)-*N*-(3-hydroxypropyl)amine, **L1** (Scheme 5).⁷ Complex **1** was thermally stable under dinitrogen atmosphere and was fully characterized by ¹H and ¹³C NMR spectroscopy, including correlated ¹H–¹H COSY, ¹H–¹H NOESY, and ¹H–¹³C HSQC and HMBC NMR spectroscopy at both room temperature and –30 °C, as well as by mass spectrometry and IR spectroscopy. The IR spectra of free ligand **L1** and complex **1** show peaks due to ν (OH) centered at 3304 and 3285 cm⁻¹, respectively. The MALDI-MS of **1** gave a parent ion peak at *m/z* = 495.9 that matches well with the simulated *m/z* value and isotope pattern for [1 + H]⁺.

Scheme 4. β -Phenyl or β -Methyl Elimination Reactions at Palladium(II)

Scheme 5. Synthesis of Complex 1 and the Proposed Mechanism of Interconversion of Isomers 1a and 1b by Way of 1*



It should be noted that complex **1** is asymmetric, so there are two potential isomers **1a** and **1b** with the CH_2Pd group *trans* to the pyridine or amine donor, respectively. However, at room temperature, the ^1H NMR spectrum of **1** in $(\text{CD}_3)_2\text{CO}$ solution gave only singlet resonances for the CH_2 and CMe_2 groups of the organic $\text{CH}_2\text{CMe}_2\text{C}_6\text{H}_4$ ligand, while four resonances for the C_6H_4 group were observed (Figure 1). Only a single set of broad resonances was observed for the two pyridylmethyl groups of coordinated ligand **L1**, suggesting that the complex might exhibit fluxionality, and this was confirmed by the NMR spectra at lower temperatures. At -30°C , each broad pyridyl resonance had split into two equal resonances. Additionally, the broad CH_2N resonance that integrates to four protons (for H7a and H7b) had split into four overlapping doublets in the region δ 4.1–4.4 (Figure 1). Similarly, the CMe_2 resonance of the organic ligand had split into two equal resonances, while the CH_2 resonance did not give resolved

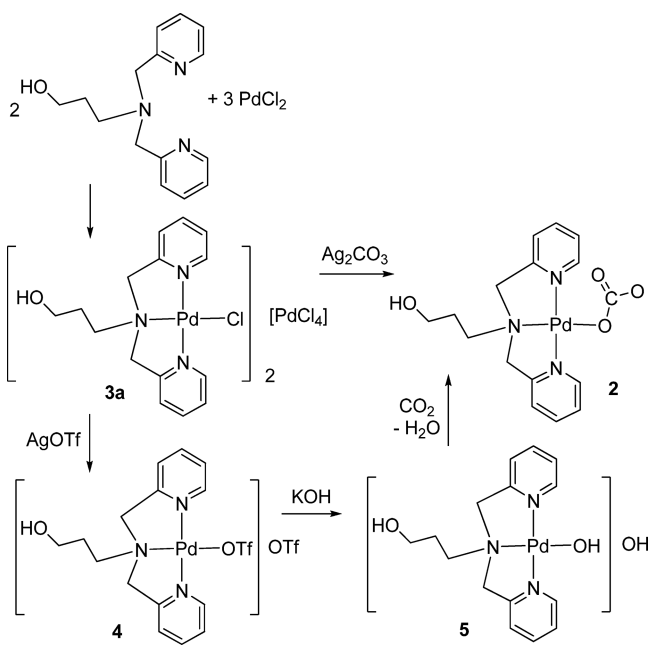
Figure 1. ^1H NMR spectra (600 MHz, acetone- d_6 solution) of complex **1** at different temperatures.

separate peaks. Following precedents on the mechanisms of substitution at palladium(II),¹⁸ it is likely that the exchange between free and coordinated pyridyl groups occurs by way of square pyramidal and trigonal bipyramidal intermediates, and the trigonal bipyramidal intermediate **1*** (which contains an effective plane of symmetry) is able to collapse to **1a** or **1b** by dissociation of one of the two pyridyl groups (Scheme 5). The activation energy for fluxionality is estimated, using the Eyring equation, as $\Delta G^\ddagger = 58 \text{ kJ mol}^{-1}$ at 297 K .^{19a}

In solution, complex **1** exists largely as one isomer, though minor peaks in the low temperature NMR spectra might be due to a minor isomer. A ^1H – ^1H NOESY experiment was carried out at -30°C to check for the close interligand contacts expected between H6a and H6 for isomer **1a** or H6a and H9 for isomer **1b**. However, no interligand correlations were observed, perhaps as a result of the fluxionality, so it is uncertain if the major isomer is **1a** or **1b**.

All attempts to crystallize **1** (dry solvent, inert atmosphere, various solvents, and temperatures) were unsuccessful. However, in one attempt, a solution of complex **1** in tetrahydrofuran, which had not been dried or distilled, was allowed to evaporate slowly in air and gave good crystals of a compound which was structurally characterized as the carbonate complex $[\text{Pd}(\kappa^1\text{-O-CO}_3)(\kappa^3\text{-N,N',N''-L1})]$, **2**, in the hydrated form $[\text{Pd}(\kappa^1\text{-O-CO}_3)(\kappa^3\text{-N,N',N''-L1})] \cdot 6\text{H}_2\text{O}$, **2a**. There were enough single crystals to obtain a ^1H NMR spectrum of complex **2**, which was soluble in D_2O . The NMR spectrum was consistent with the observed structure, in which both pyridyl groups are coordinated and the complex has approximate C_s symmetry. However, there was insufficient material to allow full characterization, and the mechanism by which the organic $\text{CH}_2\text{CMe}_2\text{C}_6\text{H}_4$ ligand was replaced by carbonate was obscure. Further research was clearly necessary. In the first step, the independent synthesis of complex **2** was carried out, as illustrated in Scheme 6. The reaction of ligand **L1** with palladium(II) chloride gave the cationic chloropalladium(II) complex $[\text{PdCl}(\kappa^3\text{-N,N',N''-L1})]^+$, **3**, which was isolated as the tetrachloropalladate(II) salt $[\text{PdCl}(\kappa^3\text{-N,N',N''-L1})][\text{PdCl}_4]$, **3a**. The chloride salt $[\text{PdCl}(\kappa^3\text{-N,N',N''-L1})]\text{Cl}$, **3b**, was prepared later. Complex **3a** reacted with excess silver carbonate to give complex **2** in good yield. Alternatively, complex **3a** reacted with silver triflate to give the triflate complex **4**, which reacted with potassium hydroxide to

Scheme 6. Two Independent Syntheses of the Palladium(II) Carbonate Complex 2



give hydroxopalladium(II) complex **5**, which could then undergo further reaction with carbon dioxide to give **2**. This last synthesis is analogous to the route used to make other bicarbonate or carbonate complexes of palladium(II) (Scheme 2)^{9–11} and provides a potential step in which CO_2 from air could give complex **2**.

Complexes **2** (both **2a** and a different crystalline form $[\text{Pd}(\kappa^1\text{-O-CO}_3)(\kappa^3\text{-N,N',N''-L1})\cdot 5\text{H}_2\text{O}\cdot \text{MeOH}$, **2b**) and **3b** were characterized by structure determination, and all complexes **2–5** were characterized spectroscopically. The ^1H and ^{13}C NMR spectra were consistent with the complexes having C_s symmetry, with equivalent 2-pyridylmethyl groups, for which each CH^aH^b group appeared as an AB multiplet in the ^1H NMR spectra. The ^{13}C NMR spectrum of complex **2** contained a resonance at $\delta = 166$ for the carbonate carbon atom, just outside the range $\delta = 159\text{--}164$ reported for η^2 -carbonate or η^1 -bicarbonate complexes of palladium(II).^{9–11} The infrared spectrum of complex **2** contained a strong band at 1316 cm^{-1} , assigned to $\nu(\text{CO})$ of the η^1 -carbonate ligand, at considerably lower energy than the range of $1655\text{--}1700\text{ cm}^{-1}$ found for η^2 -carbonate complexes^{9–11,19b} or $1600\text{--}1650\text{ cm}^{-1}$ found for η^1 -bicarbonate complexes,^{9,10} indicating that this could be a useful criterion to distinguish between these bonding modes. In the MALDI-MS of **2**, using an anthracene matrix containing KCl to aid ionization, the most abundant ion was observed at m/z 462.8, corresponding to $[2 + \text{K}]^+$ (Figure 2).

The structure of complex **3b** is shown in Figure 3 and confirms that **L1** acts as a tridentate ligand binding through the three nitrogen donors to give a square planar cationic palladium(II) complex. The bond length $\text{Pd}\text{--}\text{N}(2)$ for the amine donor is slightly longer than those to the pyridine donors, and the distances are unexceptional.²⁰ The hydroxyl group is not coordinated but is hydrogen bonded to both the chloride anion and a water molecule in **3b**. Complex **3b** forms an interesting supramolecular polymeric structure formed by hydrogen bonding between the CH_2OH group, chloride anion and two water molecules, as illustrated in Figure S40.

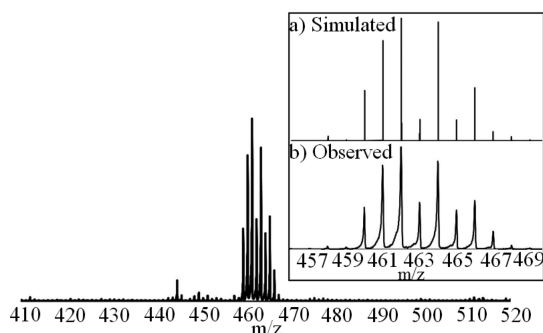


Figure 2. Isotope patterns for $[2 + \text{K}]^+$: (a) simulated and (b) observed by MALDI MS using anthracene as the matrix.

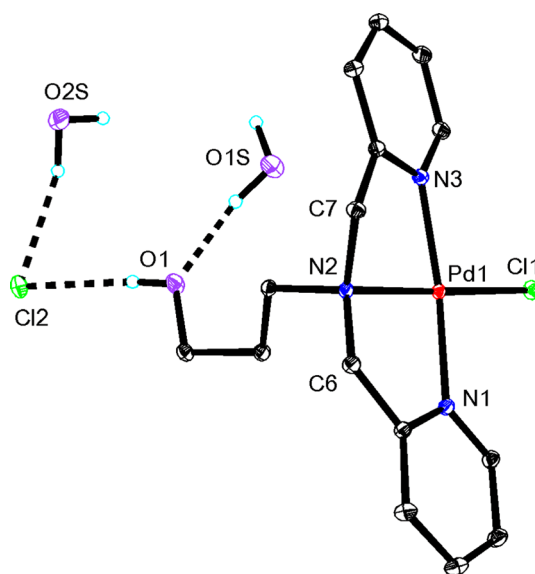


Figure 3. Structure of complex **3b**, showing 30% probability ellipsoids. Selected bond distances (Å): $\text{Pd}(1)\text{--}\text{N}(1)$ 2.0170(8); $\text{Pd}(1)\text{--}\text{N}(2)$ 2.0254(8); $\text{Pd}(1)\text{--}\text{N}(3)$ 2.0107(8); $\text{Pd}(1)\text{--}\text{Cl}(1)$ 2.3024(6).

The molecular structures of complex **2** in solvates **2a** and **2b** are shown in Figure 4. The ligand is bound in a similar way as in complex **3**, and all contain slightly distorted square planar palladium(II) centers, with Houser's parameter $\tau_4 = 0.10$, 0.09, and 0.13 in **2a**, **2b**, and **3** respectively.²¹ The carbonate ligand is oriented roughly perpendicular to the square plane of the palladium(II) center and *syn* to the 3-hydroxypropyl group in each case. The carbonate is clearly monodentate, and to the best of our knowledge, this is the first example of a palladium complex containing a carbonate ligand bound in this form. The key to its formation is likely to be the use of a neutral pincer ligand that both prevents carbonate chelation and gives a neutral complex. With monodentate or bidentate coligands, bidentate carbonate is usually preferred (**K**, Scheme 2), while with anionic pincer ligands, the monodentate bicarbonate or bridging carbonate (**M** and **N**, Scheme 2) is preferred.^{9–11} The main difference between the molecular structures of **2a** and **2b** is in the conformation of the 3-hydroxypropyl substituents, and this is attributed to different hydrogen bonding in the two solvates.

Both complexes **2a** and **2b** give complex three-dimensional network structures by hydrogen bonding involving the carbonate ligands, the 3-hydroxypropyl groups, and water molecules. Figure 5 shows a small part of these networks in

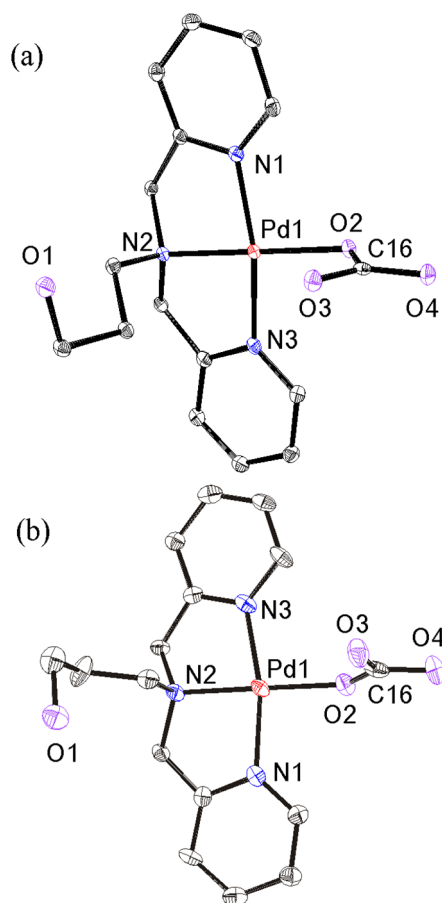


Figure 4. Molecular structures of complexes (a) **2a** and (b) **2b**, showing 30% probability ellipsoids. Selected bond distances (Å) and angles (deg): **2a**, Pd(1)–N(1) 2.003(9); Pd(1)–N(2) 2.007(8); Pd(1)–N(3) 2.007(9); Pd(1)–O(2) 2.012(7); C(16)–O(2) 1.221(13); C(16)–O(4) 1.352(13); C(16)–O(3) 1.258(12); N(1)–Pd(1)–N(2) 84.27(3); N(2)–Pd(1)–N(3) 82.99(3); N(3)–Pd(1)–O(2) 97.06(3); O(2)–Pd(1)–N(1) 95.52(3); **2b**, Pd(1)–N(1) 2.006(2); Pd(1)–N(2) 2.017(2); Pd(1)–N(3) 2.015(2); Pd(1)–O(2) 2.020(2); C(16)–O(2) 1.325(3); C(16)–O(4) 1.285(3); C(16)–O(3) 1.256(3); N(1)–Pd(1)–N(2) 83.46(9); N(2)–Pd(1)–N(3) 84.00(9); N(3)–Pd(1)–O(2) 96.49(8); O(2)–Pd(1)–N(1) 96.10(8).

which dimer units can be identified. In complex **2a**, there is direct pairwise intermolecular H-bonding between the carbonate and alcohol groups, with O(1)⋯O(4A) = O(1A)⋯O(4) = 2.67 Å, while pairs of water molecules also bridge between carbonate ligands, with O(3)⋯O(5) = O(3A)⋯O(5A) = 2.71 Å and O(3)⋯O(5a) = O(3a)⋯O(5) = 2.80 Å. In complex **2b**, a water molecule O(2W) bridges between each carbonate and alcohol group, with O(1)⋯O(2WA) = O(1A)⋯O(2W) = 2.74 Å and O(3)⋯O(2W) = O(3a)⋯O(2WA) = 2.70 Å.

Having proved the structure of unusual carbonate complex **2**, the remaining challenge was to determine how it was formed from complex **1**. It seemed possible that this could involve reaction of **1** with some combination of water, dioxygen, and carbon dioxide. No reaction occurred when a solution of complex **1** in dry tetrahydrofuran was stirred under CO₂, O₂, or a combination of the two. However, a reaction did occur when a solution of **1** in wet tetrahydrofuran was stirred under an atmosphere of CO₂ to give cationic neophylpalladium(II) complex **6** as the bicarbonate salt (Scheme 7). The ¹H NMR

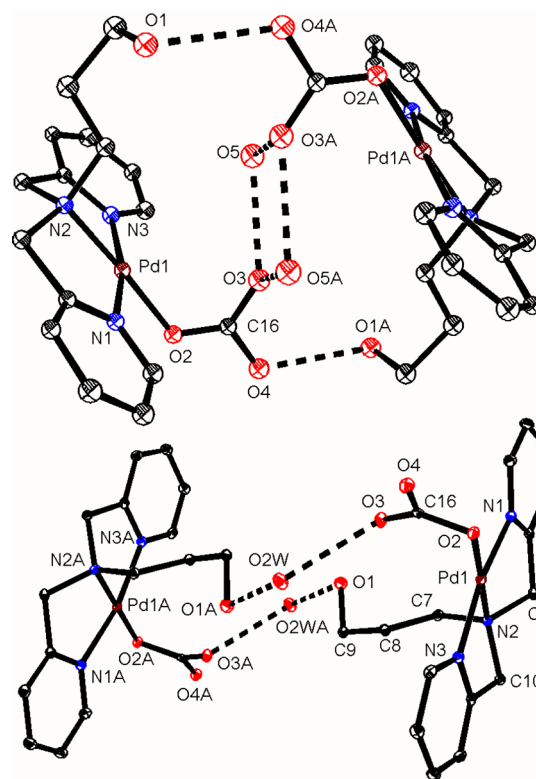
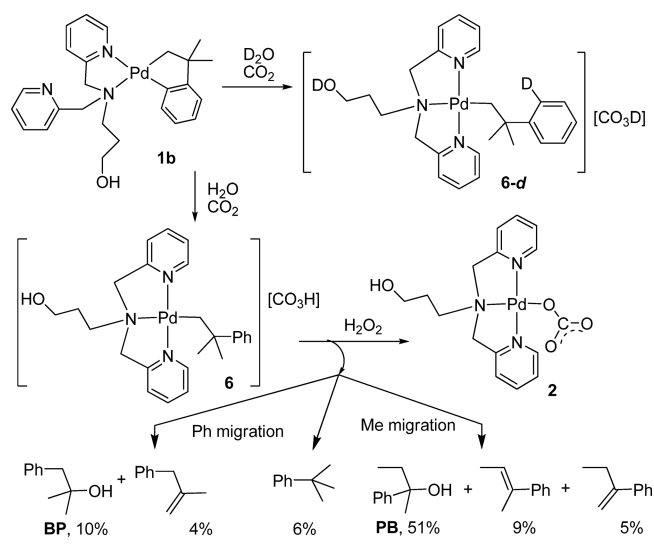


Figure 5. Structures of dimer units of (above) complex **2a** and (below) complex **2b** formed by hydrogen bonding, showing 25% thermal ellipsoids.

Scheme 7. Conversion of Complex **1** to **2** by Way of Complex **6** and the Distribution of Organic Products



spectrum of **6** showed the resonances expected for the ligand in $\kappa^3\text{-N}_3\text{N}'\text{N}''\text{-L1}$ bonding mode, similar to those for complexes **2**–**5** and also peaks typical for the neophylpalladium group.^{2,5,6} In particular, the phenyl group gave three resonances in a 2:2:1 intensity ratio for the *o*-, *m*-, and *p*-H atoms. When the similar reaction was carried out in D₂O, the corresponding complex **6-d** was formed (Scheme 7), in which the phenyl group contained one deuterium atom in the *ortho* position, as shown by the ¹H and ²H NMR spectra (Figure 6). In particular, the *ortho* resonance in the ¹H NMR integrated as a single proton, and the

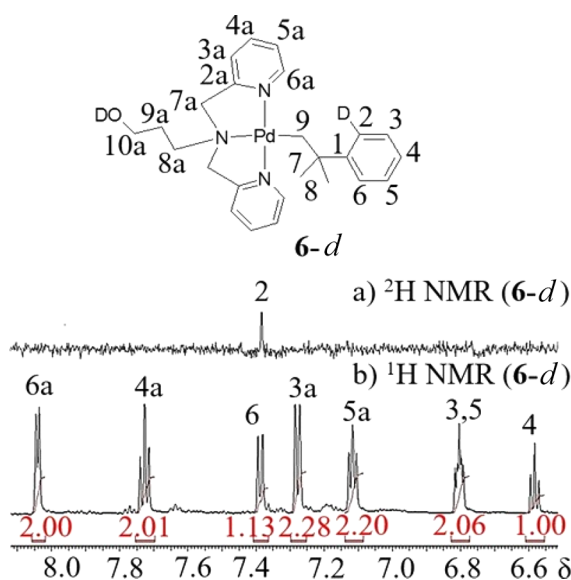


Figure 6. NMR spectra of complex **6-d** in D_2O solution: (a) 2H NMR spectrum and (b) 1H NMR spectrum.

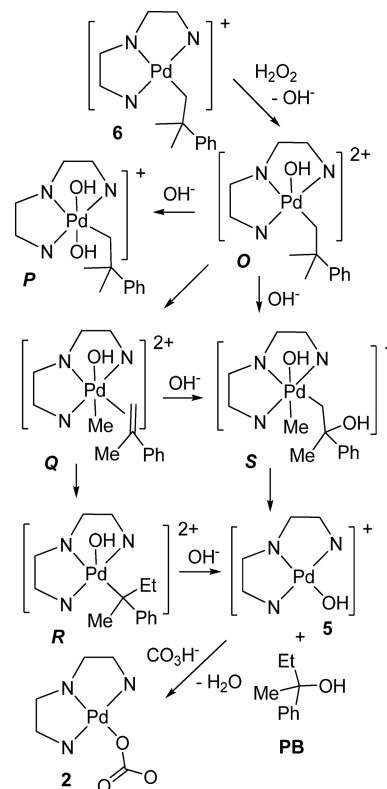
2H NMR showed the presence of an *ortho*-D atom. In the infrared spectrum of complex **6**, a strong band was observed at $\nu(CO) = 1611\text{ cm}^{-1}$, which is in the range for the bicarbonate ion ($1610\text{--}1655\text{ cm}^{-1}$).^{19b} The formation of **6** from **1** involves selective protonolysis of the aryl-palladium bond by carbonic acid,^{5,6} but further protonolysis of the Pd-neophyl group from **6** did not occur under these conditions. An attempt to recrystallize complex **6** from chloroform led to decomposition to give chloro complex **3b** (Figure 3). The reaction of **6** with DCl in D_2O solution also gave complex **3b** along with $PhCMe_2CH_2D$. Finally, it was hypothesized that peroxide impurity in the tetrahydrofuran solvent might have been involved in the original synthesis of complex **2**, so a reaction of complex **6** in aqueous solution with hydrogen peroxide was carried out. This reaction did indeed give complex **2** in good yield.

The complex mixture of organic products from the reaction of complex **6** in D_2O solution with H_2O_2 was analyzed after extraction into $CDCl_3$ by a combination of GC-MS and 1H NMR spectroscopy.²² The major organic products were identified as $PhMeEtCOH$ (2-phenyl-2-butanol, **PB**, 51%), *trans*- $PhMeC=CHMe$ (*trans*-2-phenyl-2-butene, 9%), and $PhEtC=CH_2$ (2-phenyl-1-butene, 5%), which are products expected for hydrolysis of a neophyl cation after methyl group migration (compare Schemes 3 and 7),¹⁴ $PhCH_2CMe_2OH$ (2-benzyl-2-propanol, **BP**, 10%) and $PhCH_2CMe=CH_2$ (2-benzyl-1-propene, 4%), which are products expected for hydrolysis of a neophyl cation after phenyl group migration (Schemes 3 and 7),¹⁴ and *t*-BuPh (*t*-butylbenzene, 6%), which is the product expected from protonolysis of the neophyl group from **6** without rearrangement. Together, these products account for 85% of the neophyl groups originally present in the reagent **6**. No neophyl dimers were detected, which would be expected if neophyl radical intermediates were involved.^{12,13} Also absent was the alcohol $PhMe_2CCH_2OH$, which would be formed by hydrolysis of the neophyl cation without rearrangement. Although the nature of the products is as expected for a neophyl cation intermediate, the selectivity is dramatically different. Thus, the reaction of Scheme 3, with neophyl rearrangement, occurs with <1% methyl migration and >99%

phenyl migration, but the present reaction occurs with 65% methyl migration and only 14% phenyl migration. A mechanism involving either a free neophyl carbocation or radical intermediate can therefore be eliminated based on the observed organic product distribution.^{12–14} The rearrangement is therefore proposed to occur within the coordination sphere of the palladium center, probably after oxidation of complex **6** by hydrogen peroxide.

Two possible routes to major products **2** and $PhMeEtCOH$, **PB**, are shown in Scheme 8, both involving β -methyl

Scheme 8. Possible Mechanisms of Reaction of **6** with H_2O_2 To Give **2**^a



^aLigand **L1** is drawn as NNN for simplicity. The favored mechanism involves concerted β -Me elimination and nucleophilic OH^- attack followed by C–C reductive elimination (**O** \rightarrow **S** \rightarrow **5**). The disfavored mechanism involves β -Me elimination, alkene insertion and C–O reductive elimination (**O** \rightarrow **Q** \rightarrow **R** \rightarrow **5**).

elimination as a key step. Hydrogen peroxide often gives *trans* oxidative addition by a polar mechanism.^{1,3,23} In reaction with complex **6** this would give dicationic hydroxopalladium(IV) intermediate **O**,^{1,3} and then octahedral palladium(IV) complex **P**. However, if hydroxide coordination to give **P** does not occur, then β -methyl elimination from **O** might occur to give alkene complex **Q**,^{15–17} which could undergo alkene insertion in the opposite sense to give $PhMeEtCPd(IV)$ intermediate **R**. Reductive elimination with C–OH bond formation could then give organic product **PB** and complex **S**, which would be expected to react easily with the bicarbonate anion to give observed product **2**. There are several difficulties with this mechanism. Alkene complexes of palladium(IV) are unknown, and dicationic complex **Q** is likely to be at high energy. Isomerization of primary alkyl complex **O** to tertiary alkyl complex **R** is also likely to be unfavorable. Finally,

reductive elimination with alkyl C–O bond formation usually occurs by external nucleophilic attack at carbon, and this will be difficult with a bulky tertiary alkyl group, as in **R**.^{4,24} Perhaps more likely is that the β -methyl elimination occurs in concert with hydroxide addition to give **S** and that **S** undergoes reductive elimination with C–C bond formation to give **5** and **PB** (Scheme 8). The minor alcohol product PhCH₂CMe₂OH (2-benzyl-2-propanol, **BP**) would be formed by an analogous sequence of reactions if the first intermediate **O** underwent β -phenyl instead of β -methyl elimination. The challenge is to understand why β -methyl elimination is dominant, when the closest precedent from palladium(II) chemistry would predict selective β -phenyl elimination (Scheme 4).^{2,24}

COMPUTATIONAL STUDIES

Several problems in the above study could not be solved experimentally, so DFT calculations (BP functional, scalar correction for relativity) were carried out to provide additional insight. The calculated structures for complexes **1a** and **1b** are shown in Figure 7. Complex **1b** is calculated to be more stable than **1a** by 7 kJ mol⁻¹, so it is tentatively assigned as the dominant isomer of complex **1** (Scheme 5).

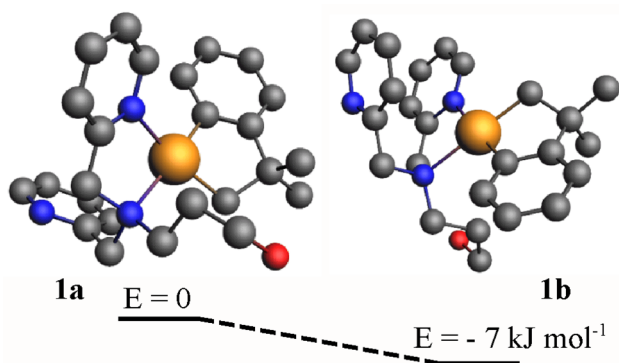


Figure 7. Calculated structures and relative energies of isomers **1a** and **1b**.

The modeling of the potential oxidative addition of hydrogen peroxide to complex **6** is shown in Figure 8. Complex **O** contains PdOH, CH₂OH and OH⁻ groups but the structure is predicted to have hydrogen bonding involving all of them.²⁵ As

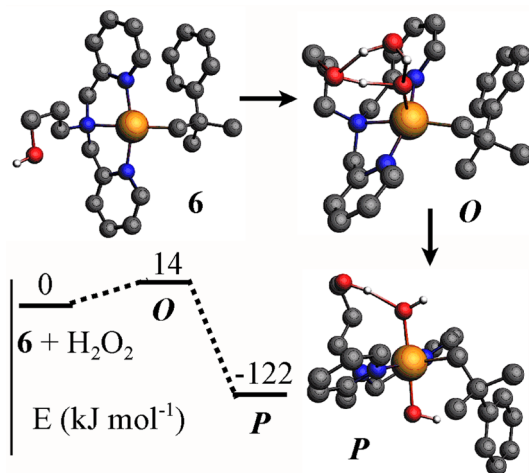


Figure 8. Calculated structures and relative energies of **6**, **O**, and **P**.

expected, octahedral palladium(IV) complex **P**, which is predicted to have hydrogen bonding between the CH₂OH and adjacent PdOH group, is calculated to be most stable, though it was not observed. One feature that may be particularly significant is that the predicted conformation of the neophyl group in **6** and **O** has π -stacking between the phenyl group and one of the 2-pyridyl groups with one methyl group oriented toward the palladium center. In order to form potential product **P**, the neophyl group has to reorient in order to allow access of the hydroxide ion to palladium (Figure 8).

We have attempted to model the potential intermediates and products arising from the unique neophyl rearrangement (Scheme 8). No minimum could be found for the potential alkene intermediate [Pd(OH)Me(CH₂=CMePh)L1]²⁺OH⁻, **Q**, or the analogous product of β -phenyl elimination, [Pd(OH)Ph(CH₂=CMe₂)L1]²⁺OH⁻, **Q***. The best structures found resembled carbocations containing the Pd-CH₂-CMePh⁺ or Pd-CH₂-CMe₂⁺ units in **Q** and **Q***, respectively, and were at high energy. Consistent with the arguments above, the potential route involving β -methyl elimination and alkene insertion to give intermediates **Q** and **R** is considered to be improbable. Figure 9 shows the calculated structures of the

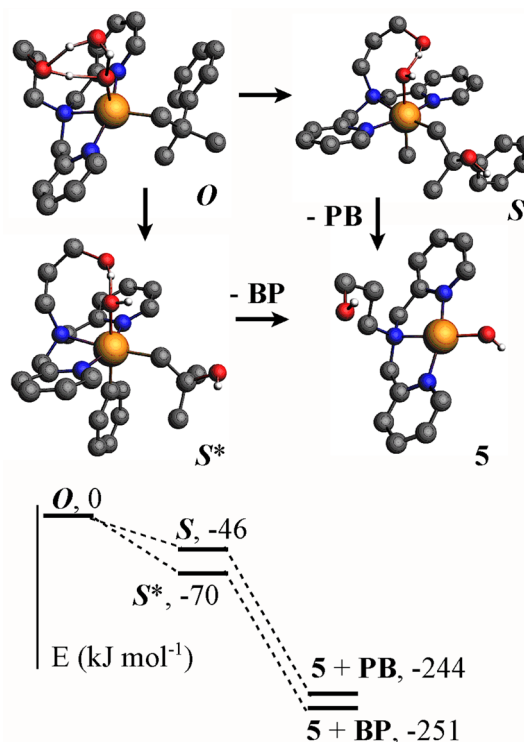


Figure 9. Predicted structures and relative energies of complexes **O**, **S**, **S***, and **5**.

potential intermediates [Pd(OH)Me(CH₂-CMePhOH)L1]⁺, **S**, and the analogous product of β -phenyl elimination, [Pd(OH)Ph(CH₂-CMe₂OH)L1]⁺, **S***, for the alternative mechanism involving concerted β -carbon elimination/hydroxide addition. The formation of **S** or **S*** and subsequent reductive elimination with C–C bond formation (probably after a ligand dissociation step)^{2,26} to form the alcohol **PB** (Scheme 8) or **BP** are favorable, so this route is considered likely. However, these limited calculations do not explain the observed selectivity since the product of phenyl migration **S*** is calculated to be more stable than that of methyl migration **S**,

and so the usual dominance of phenyl migration in neophyl rearrangements or β -carbon elimination, based on the better bridging ability of the phenyl group, might be predicted.^{14,15} A possible explanation is that the initial oxidation step to give **O**, in which a methyl group is oriented close to palladium (Figure 9), is rate-determining and that methyl group migration occurs somewhat faster than the rotation about the neophyl-palladium bond that is needed to orient the phenyl group close to the vacant site, as required for phenyl group migration. Rotation of the neophyl group will be slowed by steric effects and also electronic effects, since the phenyl/pyridine π -stacking attraction will be lost on rotation. We know of no precedents for β -elimination at palladium(IV), but there are examples of remote methyl group migration to platinum(IV) from methylboron or methylsilicon groups, often initiated by nucleophilic attack by hydroxide at boron or silicon.^{17,24}

The observed structures of complex **2** exhibit complex hydrogen bonding motifs (Figure 5). The complex is formulated as a neutral carbonate complex, in which the carbonate group is hydrogen bonded to water and, in **2a**, to the alcohol substituent. The hydrogen atoms were not refined in the structure determinations, and calculations on some model compounds were carried out to probe the nature of these hydrogen bonding interactions. In the three cases studied (Figure 10), an unsymmetrical hydrogen bond O–H...O is

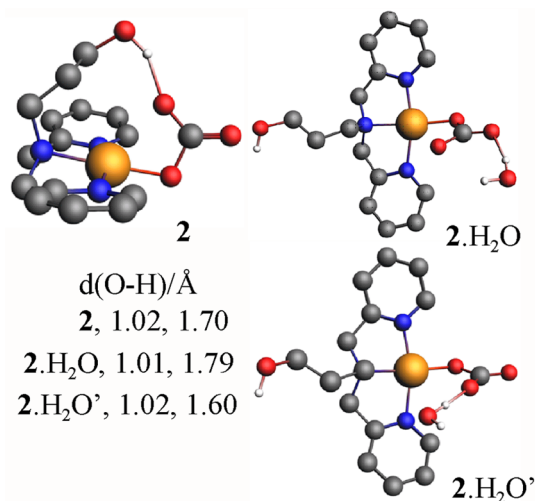


Figure 10. Calculated hydrogen bonded structures for complex **2**. In the O–H...O units, the shorter OH distance is to the oxygen of water or alcohol, and the longer distance is to the oxygen of carbonate.

predicted with the longer distance to the carbonate oxygen atom. This is the expected pattern given the relative base strengths of RO⁻, OH⁻, and CO₃²⁻ and supports the proposed formulation of complex **2** as the first monodentate carbonate complex of palladium(II).

CONCLUSIONS

A palladium(II) complex **2** containing a monodentate carbonate ligand was first prepared serendipitously, by fixation of carbon dioxide from air during an attempt to recrystallize a new fluxional “cycloneophyl” complex, **1**.^{1–4} The reaction is shown to occur in two steps. The first involves protonolysis by H₂O/CO₂ of the arylpalladium bond of **1** to give a cationic neophylpalladium complex with a bicarbonate anion. The second step involves oxidation of this complex by peroxide

(perhaps present in the original synthesis as an impurity in the tetrahydrofuran solvent). This oxidation step is followed rapidly by formation of complex **2** with release of a mixture of organic products, the major one being 2-phenyl-2-butanol, **PB**. The formation of **PB** involves a neophyl rearrangement with the unprecedented preference for methyl over phenyl migration. A possible mechanistic basis for this unexpected reaction is proposed, involving β -carbon elimination at a palladium(IV) center.

EXPERIMENTAL SECTION

General Procedures. Reactions were carried out in air, unless otherwise specified. For those reactions that were conducted under a nitrogen atmosphere, standard Schlenk or glovebox techniques were used. All solvents used for air- and moisture-sensitive reactions were purified using an Innovative Technologies 400–5 Solvent Purification System (SPS) and were stored over activated 4 Å molecular sieves. NMR spectra were recorded at 298 K using a Varian 600 MHz spectrometer (¹³C at 150.7 MHz). ¹H and ¹³C chemical shifts are reported relative to TMS. Complete assignments were aided by the use of ¹H–¹H gCOSY, ¹H–¹H NOESY, ¹H–¹³C{¹H} HSQC, and ¹H–¹³C{¹H} HMBC experiments and are reported using the labeling scheme in Figures 1 and 6 and in the Supporting Information. For ²H NMR experiments, ²H chemical shifts were referenced externally to the ²H peak of D₂O ($\delta(^2\text{H}) = 4.63$ ppm). Aqueous 30% H₂O₂ was degassed by bubbling N₂ through for 10 min. Complexes [PdCl₂(COD)], [Pd(CH₂CMe₂C₆H₄)(COD)], and the ligand, *N,N*-bis(pyrid-2-ylmethyl)-*N*-(2-hydroxyethyl)amine, **L1**, were synthesized according to the literature procedures.^{2,5–7} NMR for **L1** in CDCl₃: $\delta(^1\text{H}) = 8.55$ (d, 2H, ³J(H5H6) = 5 Hz, H6), 7.63 (t, 2H, ³J(H3H4) = ³J(H4H5) = 8 Hz, H4), 7.40 (d, 2H, ³J(H3H4) = 8 Hz, H3), 7.16 (dd, 2H, ³J(H4H5) = 8 Hz, 5 Hz, H5), 3.81 (s, 4H, CH₂N), 3.73 (t, 2H, ³J(HH) = 6 Hz, CH₂O), 2.76 (t, 2H, ³J(HH) = 6 Hz, CH₂N), 1.79 (quin, 2H, ³J(HH) = 6 Hz, CH₂). The chemical shifts reported for **L1** in ref 7 are correct, but many of the coupling constants are not. Elemental analyses were performed by Laboratoire d'Analyse Élémentaire de l'Université de Montréal and Canadian Microanalytical Service, Ltd. MALDI-TOF mass spectra were collected using an AB Sciex 5800 TOF/TOF mass spectrometer using pyrene or anthracene as the matrix in a 20:1 matrix/substrate molar ratio. Organic products were analyzed using a Shimadzu GCMS-QP2010 Ultra GC with a DB-5 column. Infrared spectra were collected by using a PerkinElmer UATR TWO FTIR spectrometer.

[Pd(CH₂CMe₂C₆H₄)(κ²-*N,N'*-**L1**)], **1**. Under N₂, a solution of *N,N*-bis(pyrid-2-ylmethyl)-*N*-(2-hydroxypropyl)amine, **L1**, (0.148 g, 0.577 mmol) in dry THF (15 mL) was added to a stirred solution of [Pd(CH₂CMe₂C₆H₄)(COD)] (0.200 g, 0.577 mmol) in dry THF (50 mL) cooled to –65 °C. The mixture was stirred and slowly warmed to room temperature over 4 h. Upon removal of the solvent under reduced pressure, a brown oil was formed which was washed with hexane (20 mL) and cold ether (10 mL). The oil was dried under vacuum, to give **1** (0.237 g, 0.477 mmol, 83%). NMR in (CD₃)₂CO at 25 °C: $\delta(^1\text{H}) = 8.50$ (br, 2H, H6a, H6b), 7.7–7.8 (m, 4H, H3a, H3b, H4a, H4b), 7.29 (m, 2H, H5a, H5b), 7.19 (m, 1H, H6), 6.78 (m, 1H, H4), 6.73 (m, 1H, H5), 6.67 (d, 1H, ³J(H3H4) = 7 Hz, H3), 4.18 (br, 4H, H7a, H7b), 3.53 (t, 2H, ³J(H8aH9a) = 5 Hz, H8a), 2.88 (t, 2H, ³J(H9aH10a) = 8 Hz, H10a), 2.31 (m, 2H, H9a), 2.02 (s, 2H, H9), 1.31 (s, 6H, H8, H8'). $\delta(^{13}\text{C}) = 167.89$ (C2), 159.62 (C1), 157.46 (C2a, C2b), 148.81 (C6a, C6b), 136.71 (C4a, C4b), 134.44 (C5), 124.87 (C3a, C3b), 123.31 (C6), 123.06 (C5a, C5b), 121.97 (C4), 121.10 (C3), 62.71 (C7a, C7b), 59.89 (C10a), 55.32 (C8a), 47.11 (C7), 43.59 (C9), 33.42 (C8, C8'), 30.70 (C9a). NMR in (CD₃)₂CO at –20 °C: $\delta(^1\text{H}) = 8.64$ (1H, H6a or H6b), 8.46 (1H, H6a or H6b), 7.78 (1H, H4a or H4b), 7.75 (1H, H4a or H4b), 7.67–7.66 (2H, H3a and H3b), 7.36 (1H, H5a or H5b), 7.31 (1H, H5a or H5b), 7.19 (1H, H6), 6.78 (1H, H4), 6.73 (1H, H5), 6.67 (1H, H3), 4.11–4.32 (4H, H7a, H7a', H7b, H7b'), 3.4–3.6 (2H, H8a, H8a'), 2.7–2.8 (2H, H10a, H10a'), 2.36 (1H, H9a or H9a'), 2.31 (1H, H9a or H9a'), 2.05

(1H, H9 or H9'), 1.96 (1H, H9 or H9'), 1.31 (3H, H8 or H8'), 1.27 (3H, H8 or H8'). MALDI MS (pyrene matrix): Calcd for [Pd(CH₂CMe₂C₆H₄)L1]⁺: *m/z* 495.9. Observed: *m/z* 495.9. IR: $\nu(\text{O}-\text{H})$ 3285 cm⁻¹. Recrystallization from unpurified THF led to decomposition, with formation of crystals of **2a**, whose ¹H NMR spectrum was identical to that of **2**, reported below.

[Pd(CO₃)(κ^3 -N,N',N''-L1)], **2**. In a darkened flask, to an aqueous solution (3 mL) of **3** (0.040 mg, 0.038 mmol) was added silver carbonate (0.031 mg, 0.11 mmol) in water (4 mL) with stirring. After 17 h, the reaction mixture was centrifuged to separate silver chloride and palladium salt as precipitates. The solvent was evaporated from the resultant yellow solution under vacuum to give **2** as an air-stable, yellow solid (0.040 mg, 0.094 mmol, 83%). NMR in D₂O: $\delta(^1\text{H})$ = 8.17 (d, 2H, ³J(H5aH6a) = 6 Hz, H6a), 8.13 (dd, 2H, ³J(H5aH6a) = 6 Hz, ³J(H4aH5a) = 7 Hz, H5a), 7.63 (d, 2H, ³J(H3aH4a) = 7 Hz, H3a), 7.58 (t, 2H, ³J(H3aH4a) = ³J(H4aH5a) = 7 Hz, H4a), 5.30 (d, 2H, ²J(H7aH7a') = 16 Hz, H7a or H7a'), 4.43 (d, 2H, ²J(H7aH7a') = 16 Hz, H7a or H7a'), 3.55 (m, 2H, H10a), 3.09 (m, 2H, H8a), 2.02 (m, 2H, H9a). $\delta(^{13}\text{C})$ = 166.85 (carbonate), 163.26 (C2a), 148.50 (C6a), 141.41 (C5a), 124.80 (C4a), 122.86 (C3a), 67.50 (C7a), 60.47 (C10a), 58.57 (C8a), 30.20 (C9a). MALDI MS (Anthracene matrix): Calcd for [Pd(CO₃)L1 + K]⁺: *m/z* = 462.8. Obsd: *m/z* = 462.8. IR $\nu(\text{O}-\text{H})$ 3341 cm⁻¹, $\nu(\text{C}-\text{O})$ 1316 cm⁻¹. Anal. Calcd for C₃₂H₄₀N₆O₈Pd₂·5H₂O: C, 40.90; H, 5.36; N, 8.94. Found: C, 41.07; H, 5.07; N 8.92. Yellow crystals suitable for single-crystal X-ray crystallographic analysis were grown by the slow evaporation of an aqueous solution of **2** at room temperature.

[PdCl(κ^3 -N,N',N''-L1)]₂[PdCl₄], **3a**. To a stirred solution of [PdCl₂(COD)] (0.300 g, 1.05 mmol) in acetone (50 mL) was added an acetone solution (20 mL) of **L1** (0.180 g, 0.700 mmol). A brown precipitate was observed after 15 min. The mixture was stirred for 2 more hours. The precipitate was then collected by vacuum filtration and washed with acetone (3 × 5 mL) and dried under vacuum, to give **3** as an air-stable solid (0.322 g, 0.307 mmol, 88%). NMR in CD₃OD: $\delta(^1\text{H})$ = 8.72 (d, 2H, ³J(HH) = 6 Hz, H6a), 8.15 (dd, 2H, ³J(HH) = 6 Hz, 7 Hz, H5a), 7.69 (d, 2H, ³J(HH) = 7 Hz, H3a), 7.57 (t, 2H, ³J(HH) = 7 Hz, H4a), 5.42 (d, 2H, ²J(HH) = 15 Hz, H7a or H7a'), 4.52 (d, 2H, ²J(HH) = 15 Hz, H7a or H7a'), 3.52 (t, 2H, ³J(HH) = 5 Hz, H10a), 3.17 (m, 2H, H8a), 1.92 (m, 2H, H9a). $\delta(^{13}\text{C})$ = 164.86 (C2a), 150.58 (C6a), 141.32 (C5a), 124.73 (C4a), 122.93 (C3a), 67.30 (C7a), 60.92 (C8a), 58.22 (C10a), 30.70 (C9a). HRMS (ESI-TOF): Calcd for [C₁₅H₁₉ClN₃OPd]⁺: *m/z* = 398.025139. Observed: *m/z* = 398.02504. IR: $\nu(\text{O}-\text{H})$ 3380 cm⁻¹. Anal. Calcd for C₃₀H₃₈Cl₆N₆O₂Pd₃: C, 34.43; H, 3.66; N, 8.03. Found: C, 34.03; H, 3.70; N 7.79. Crystals were obtained by slow evaporation of a solution of **3** in methanol at room temperature, and the connectivity was established (Figure S39, CCDC 1570681), though disorder of the [PdCl₄]²⁻ unit and associated water solvate molecules did not allow full refinement.

[Pd(OTf)(κ^3 -N,N',N''-L1)](OTf), **4**. In a darkened flask, an aqueous solution (2 mL) of silver triflate (0.058 mg, 0.228 mmol) was added to a solution of **3** (0.040 mg, 0.038 mmol) in water (5 mL). The mixture was stirred for 20 min, then centrifuged to separate insoluble material. The solvent was evaporated under vacuum from the light brown solution to give **4** in 82% yield (0.083 mg, 0.062 mmol). NMR in D₂O: $\delta(^1\text{H})$ = 8.04 (m, 4H, H5a, H6a), 7.53 (d, 2H, ³J(HH) = 8 Hz, H3a), 7.47 (t, 2H, ³J(HH) = 8 Hz, H4a), 5.52 (d, 2H, ³J(HH) = 15 Hz, H7a or H7a'), 4.32 (d, 2H, ³J(HH) = 15 Hz, H7a or H7a'), 3.41 (t, ³J(HH) = 6 Hz, 2H, H10a), 3.00 (m, 2H, H8a), 1.87 (m, 2H, H9a). $\delta(^{13}\text{C})$ = 163.13 (C2a), 148.70 (C5a), 142.18 (C6a), 124.96 (C4a), 123.07 (C3a), 118.49 (CF₃), 68.61 (C7a), 61.53 (C8a), 58.33 (C10a), 30.15 (C9a); $\delta(^{19}\text{F})$ = -78.96. HRMS (ESI-TOF): Calcd for [C₁₆H₁₉F₃N₃O₄PdS]⁺: *m/z* = 512.00832. Observed: *m/z* = 512.00854. IR: $\nu(\text{O}-\text{H})$ 3303 cm⁻¹.

[Pd(OH)(κ^3 -N,N',N''-L1)](OH), **5**. To a solution of **4** (0.05 mg, 0.037 mmol) in water (10 mL) was added an aqueous solution (3 mL) of KOH (0.008 mg, 0.151 mmol) while stirring. After 20 min, the reaction mixture was centrifuged. The light brown solution was dried under vacuum to give a brown powder in 85% yield (0.025 mg, 0.060 mmol). NMR in D₂O: $\delta(^1\text{H})$ = 8.13 (m, 2H, H3a), 8.00 (t, 2H,

³J(H4aH5a) = ³J(H5aH6a) = 7 Hz, H5a), 7.50 (d, 2H, ³J(H5aH6a) = 7 Hz, H6a), 7.46 (m, 2H, H4a), 5.12 (m, 2H, H7a or H7a'), 4.28 (m, 2H, H7a or H7a'), 3.39 (t, ³J(H9aH10a) = 6 Hz, 2H, H10a), 2.88 (m, 2H, H8a), 1.79 (m, 2H, H9a). $\delta(^{13}\text{C})$ = 163.48 (C2a), 148.51 (C3a), 141.56 (C5a), 124.59 (C4a), 124.80 (C6a), 67.35 (C7a), 60.14 (C8a), 58.50 (C10a), 30.20 (C9a). MALDI MS (Pyrene matrix): Calcd for [PdL1]⁺: *m/z* 363.75. Observed: *m/z* 363.75. IR $\nu(\text{O}-\text{H})$ 3533 cm⁻¹.

[Pd(CH₂CMe₂Ph)(κ^3 -N,N',N''-L1)](HCO₃), **6**. Under N₂, degassed water (1.90 mL) was added to a dry and degassed THF solution (3 mL) of complex **1** (0.055 g, 0.11 mmol). The solution was stirred under an atmosphere of carbon dioxide for 2 h; then, the solvent was evaporated under vacuum to give **2** as a yellow powder (0.053 g, 0.096 mmol, 88%). NMR in D₂O: $\delta(^1\text{H})$ = 8.04 (d, 2H, ³J(H5aH6a) = 5 Hz, H6a), 7.73 (t, 2H, ³J(H3aH4a) = ³J(H4aH5a) = 8 Hz, H4a), 7.38 (d, 2H, ³J(HH) = 8 Hz, H2, H6), 7.27 (d, 2H, ³J(H3aH4a) = 8 Hz, H3a), 7.12 (dd, 2H, ³J(H5aH6a) = 5 Hz, ³J(H4aH5a) = 8 Hz, H5a), 6.80 (m, 2H, H3, H5), 6.58 (t, 1H, ³J(H3H4) = ³J(H4H5) = 7 Hz, H4), 4.52 (d, 2H, ²J(H7aH7a') = 15 Hz, H7a or H7a'), 4.02 (d, 2H, ²J(H7aH7a') = 15 Hz, H7a or H7a'), 3.15 (t, 2H, ³J(H9aH10a) = 6 Hz, H10a), 2.49 (m, 2H, H8a), 1.82 (s, 2H, H9), 1.29 (m, 2H, H9a), 1.19 (s, 6H, H8). $\delta(^{13}\text{C})$ = 163.84 (C2a), 160.08 (bicarbonate), 151.11 (C1), 149.33 (C6a), 139.52 (C4a), 127.66 (C3, C5), 125.70 (C2, C6), 125.28 (C4), 124.12 (C5a), 123.22 (C3a), 63.71 (C7a), 58.88 (C10a), 54.62 (C8a), 48.91 (C9), 41.46 (C7), 29.92 (C8), 29.25 (C9a). HRMS (ESI-TOF): Calcd for [Pd(CH₂CMe₂Ph)(L1)]⁺: *m/z* 496.15801. Observed: *m/z* 496.16280. IR: $\nu(\text{O}-\text{H})$ 3209 cm⁻¹, $\nu(\text{C}-\text{O})$ 1606 cm⁻¹. Anal. Calcd for C₂₆H₃₃N₃O₄Pd: C, 55.97; H, 5.96; N, 7.53. Found: C, 55.62; H, 5.93; N, 7.03. For the sample used for the ²H NMR experiment, degassed water was replaced with degassed D₂O, while the rest of the reaction conditions were unchanged. NMR in H₂O: $\delta(^2\text{H})$ = 7.4 (br, D2). Attempted recrystallization of **6** from CHCl₃ gave crystals of [PdCl(κ^3 -N,N',N''-L1)]Cl·2H₂O, **3b**, identified by structure determination.

Reaction of Complex 6 with H₂O₂. H₂O₂ (0.137 mL, 30% aqueous solution, 15 equiv) was added to a solution of complex **6** (0.055 g, 0.098 mmol) in D₂O (1.2 mL) while vigorously stirring. The solution was stirred for 3 min, then extracted with CDCl₃ (1.5 mL). The D₂O layer was shown to contain complex **2** (84%) by ¹H NMR spectroscopy. The organic layer was analyzed by GC-MS and by ¹H NMR, using 1,3,5-trimethoxybenzene as internal standard. The major product was identified as PhMeEtCOH, **PB**. Yield 51%. NMR in CDCl₃: $\delta(^1\text{H})$ = 7.43 (2H, H^a), 7.32 (2H, H^m), 7.25 (1H, H^p), 1.75–1.85 (m, 2H, MeCH^aH^b), 1.50 (s, 3H, CH₃), 0.75 (t, 3H, J = 7 Hz, CH₂CH₃).^{22a} MS: Calcd for C₁₀H₁₄O: *m/z* = 150.11. Found: *m/z* = 150.10. Other organic products were identified and analyzed similarly. All yields are an average of two runs. *trans*-2-Phenyl-2-butene (9%): NMR: $\delta(^1\text{H})$ = 7.41–7.20 (m, 5H, ArH); 5.90 (br, 1H, C=CH); 2.06 (br, 3H, Ar–C–CH₃); 1.82 (br, 3H, C=CCH₃).^{22b} MS: Calcd for C₁₀H₁₂: *m/z* = 132.20. Found: *m/z* = 132.10. 2-Phenyl-1-butene (5%): NMR: $\delta(^1\text{H})$ = 7.41–7.22 (m, 5H, ArH), 5.26 (br, 1H, =CH₂), 5.04 (br, 1H, =CH₂), 2.50 (q, 2H, CH₂), 1.09 (t, 3H, CH₃).^{22c} MS: Calcd for C₁₀H₁₂: *m/z* = 132.20. Found: *m/z* = 132.24. 2-Benzyl-2-propanol (10%): NMR: $\delta(^1\text{H})$ = 7.45–7.03 (m, 5H, ArH), 2.74 (s, 2H, CH₂), 1.2 (s, 6H, CH₃).^{22d} MS: Calcd for C₁₀H₁₄O: *m/z* = 150.11. Found: *m/z* = 150.05. 2-Benzyl-1-propene (4%): NMR: $\delta(^1\text{H})$ = 7.28–7.16 (m, 5H, ArH), 4.80 (s, 1H, =CHH), 4.72 (s, 1H, =CHH), 3.30 (s, 2H, CH₂), 1.66 (s, 3H, CH₃).^{22e} MS: Calcd for C₁₀H₁₂: *m/z* = 132.20. Found: *m/z* = 132.10. *t*-Butylbenzene (6%): NMR: $\delta(^1\text{H})$ = 7.01–7.46 (m, ArH), 1.31 (s, (CH₃)₃).^{22f} MS: Calcd for C₁₀H₁₄: *m/z* = 134.21. Found: *m/z* = 134.17. The *t*-butylbenzene-*d*₁ formed from **6** and DCl in D₂O gave MS: Calcd for C₁₀H₁₃D: *m/z* = 135.12. Found: *m/z* = 135.10.

X-ray Structure Determinations.²⁷ **Data Collection and Processing.** A crystal was mounted on a Mitegen polyimide micromount with a small amount of Paratone N oil. All X-ray measurements were made using a Bruker Kappa Axis Apex2 diffractometer at a temperature of 110 K. The frame integration was performed using SAINT, and the resulting raw data was scaled and absorption corrected using a multiscan averaging of symmetry equivalent data using SADABS.

Structure Solution and Refinement. The structures were solved by using the SHELXT program. All non-hydrogen atoms were obtained from the initial solution. The hydrogen atoms were introduced at idealized positions and were allowed to ride on the parent atom. The structural model was fit to the data using full matrix least-squares based on F^2 . The calculated structure factors included corrections for anomalous dispersion from the usual tabulation. The structure was refined using the SHELXL-2014 program from the SHELX suite of crystallographic software.²⁷ Details are given in Table S1 and in CCDC 1570679–1570682.

DFT Calculations. DFT calculations were carried out for gas phase structures by using the Amsterdam Density Functional program based on the BP functional, with double- ζ basis set and first-order scalar relativistic corrections.²⁸ Minima were confirmed by vibrational analysis; transition states were not determined. Details are given in the Supporting Information.

■ ASSOCIATED CONTENT

Supporting Information

The Supporting Information is available free of charge on the ACS Publications website at DOI: 10.1021/acs.organomet.7b00631.

Spectra and structures of the complexes; summary of X-ray data for complexes **2a**, **2b**, and **3b** (PDF)

Atomic coordinates of calculated structures (XYZ)

Accession Codes

CCDC 1570679–1570682 contain the supplementary crystallographic data for this paper. These data can be obtained free of charge via www.ccdc.cam.ac.uk/data_request/cif, or by emailing data_request@ccdc.cam.ac.uk, or by contacting The Cambridge Crystallographic Data Centre, 12 Union Road, Cambridge CB2 1EZ, UK; fax: +44 1223 336033.

■ AUTHOR INFORMATION

Corresponding Authors

*E-mail: johanna.blacquiere@uwo.ca.

*E-mail: pudd@uwo.ca.

ORCID

Richard J. Puddephatt: 0000-0002-9846-3075

Notes

The authors declare no competing financial interest.

■ ACKNOWLEDGMENTS

We thank the NSERC (Canada) for financial support.

■ REFERENCES

- (1) (a) Punniyamurthy, T.; Velusamy, S.; Iqbal, J. *Chem. Rev.* **2005**, *105*, 2329–2364. (b) Shi, Z.; Zhang, C.; Tang, C.; Jiao, N. *Chem. Soc. Rev.* **2012**, *41*, 3381–3430. (c) Stahl, S. S. *Science* **2005**, *309*, 1824–1826. (d) Shteinman, A. A. *J. Mol. Catal. A: Chem.* **2017**, *426*, 305–315. (e) Gunsalus, N. J.; Koppaka, A.; Park, S. H.; Bischof, S. M.; Hashiguchi, B. G.; Periana, R. A. *Chem. Rev.* **2017**, *117*, 8521–8573. (f) Wu, W.; Jiang, H. *Acc. Chem. Res.* **2012**, *45*, 1736–1748. (g) Campbell, A. N.; Stahl, S. S. *Acc. Chem. Res.* **2012**, *45*, 851–863. (h) Gligorich, K. M.; Sigman, M. S. *Chem. Commun.* **2009**, 3854–3867. (i) Sigman, M. S.; Jensen, D. R. *Acc. Chem. Res.* **2006**, *39*, 221–229. (j) Zhang, Y.-H.; Yu, J.-Q. *J. Am. Chem. Soc.* **2009**, *131*, 14654–14655. (k) Huang, J.; Li, J.; Zheng, J.; Wu, W.; Hu, W.; Ouyang, L.; Jiang, H. *Org. Lett.* **2017**, *19*, 3354–3357. (l) Scheuermann, M. L.; Goldberg, K. I. *Chem. - Eur. J.* **2014**, *20*, 14556–14568. (m) Vedernikov, A. N. *Acc. Chem. Res.* **2012**, *45*, 803–813.
- (2) (a) Khusnutdinova, J. R.; Rath, N. P.; Mirica, L. M. *J. Am. Chem. Soc.* **2012**, *134*, 2414–2422. (b) Qu, F.; Khusnutdinova, J. R.; Rath, N. P.; Mirica, L. M. *Chem. Commun.* **2014**, *50*, 3036–3039. (c) Behnia,

A.; Boyle, P. D.; Blacquiere, J. M.; Puddephatt, R. J. *Organometallics* **2016**, *35*, 2645–2654.

(3) (a) Thompson, K. A.; Kadwell, C.; Boyle, P. D.; Puddephatt, R. J. *J. Organomet. Chem.* **2017**, *829*, 22–30. (b) Moustafa, M. E.; Boyle, P. D.; Puddephatt, R. J. *Chem. Commun.* **2015**, *51*, 10334–10336.

(4) (a) Warren, J. J.; Tronic, T. A.; Mayer, J. M. *Chem. Rev.* **2010**, *110*, 6961–7001. (b) Weinberg, D. R.; Gagliardi, C. J.; Hull, J. F.; Murphy, C. F.; Kent, C. A.; Westlake, B. C.; Paul, A.; Ess, D. H.; McCafferty, D. G.; Meyer, T. J. *Chem. Rev.* **2012**, *112*, 4016–4093. (c) Hammes-Schiffer, S. *J. Am. Chem. Soc.* **2015**, *137*, 8860–8871. (d) Lubitz, W.; Ogata, H.; Rudiger, O.; Reijerse, E. *Chem. Rev.* **2014**, *114*, 4081–4148.

(5) (a) Cámpora, J.; López, J. A.; Palma, P.; Valerga, P.; Spillner, E.; Carmona, E. *Angew. Chem., Int. Ed.* **1999**, *38*, 147–151. (b) Cámpora, J.; Palma, P.; Carmona, E. *Coord. Chem. Rev.* **1999**, *193–195*, 207–281. (c) Cámpora, J.; Palma, P.; del Río, D.; Carmona, E.; Graiff, C.; Tiripicchio, A. *Organometallics* **2003**, *22*, 3345–3347. (d) Behnia, A.; Boyle, P. D.; Fard, M. A.; Blacquiere, J. M.; Puddephatt, R. J. *Dalton Trans.* **2016**, *45*, 19485–19490.

(6) (a) Pendleton, I. M.; Pérez-Temprano, M. H.; Sanford, M. S.; Zimmerman, P. M. *J. Am. Chem. Soc.* **2016**, *138*, 6049–6060. (b) Pérez-Temprano, M. H.; Racowski, J. M.; Kampf, J. W.; Sanford, M. S. *J. Am. Chem. Soc.* **2014**, *136*, 4097–4100. (c) Canty, A. J.; Ariafard, A.; Camasso, N. M.; Higgs, A. T.; Yates, B. F.; Sanford, M. S. *Dalton Trans.* **2017**, *46*, 3742–3748.

(7) Sundaravel, K.; Sankaralingam, M.; Suresh, E.; Palaniandavar, M. *Dalton Trans.* **2011**, *40*, 8444–8458.

(8) (a) Appel, A. M.; Bercaw, J. E.; Bocarsly, A. B.; Dobbek, H.; DuBois, D. L.; Dupuis, M.; Ferry, J. G.; Fujita, E.; Hille, R.; Kenis, P. J. A.; Kerfeld, C. A.; Morris, R. H.; Peden, C. H. F.; Portis, A. R.; Ragsdale, S. W.; Rauchfuss, T. B.; Reek, J. N. H.; Seefeldt, L. C.; Thauer, R. K.; Waldrop, G. L. *Chem. Rev.* **2013**, *113*, 6621–6658. (b) Omae, I. *Curr. Org. Chem.* **2016**, *20*, 953–962. (c) Omae, I. *Coord. Chem. Rev.* **2012**, *256*, 1384–1405. (d) Yu, D.; Teong, S. P.; Zhang, Y. *Coord. Chem. Rev.* **2015**, *293–294*, 279–291. (e) Johnson, M. T.; Wendt, O. F. *J. Organomet. Chem.* **2014**, *751*, 213–220. (f) Lau, K.-C.; Petro, B. J.; Bontemps, S.; Jordan, R. F. *Organometallics* **2013**, *32*, 6895–6898.

(9) Ariyananda, P. W. G.; Yap, G. P. A.; Rosenthal, J. *Dalton Trans.* **2012**, *41*, 7977–7983.

(10) (a) Pushkar, J.; Wendt, O. F. *Inorg. Chim. Acta* **2004**, *357*, 1295–1298. (b) Johansson, R.; Wendt, O. F. *Organometallics* **2007**, *26*, 2426–2430. (c) Mousa, A. H.; Fleckhaus, A.; Kondrashov, M.; Wendt, O. F. *J. Organomet. Chem.* **2017**, *845*, 157–164.

(11) (a) Fulmer, G. R.; Kaminsky, W.; Kemp, R. A.; Goldberg, K. I. *Organometallics* **2011**, *30*, 1627–1636. (b) Smoll, K. A.; Kaminsky, W.; Goldberg, K. I. *Organometallics* **2017**, *36*, 1213–1216. (c) Ortiz, D.; Blug, M.; Le Goff, X.-F.; Le Floch, P.; Mezailles, N.; Maitre, P. *Organometallics* **2012**, *31*, 5975–5978. (d) Ruiz, J.; Martinez, M. T.; Florenciano, F.; Rodriguez, V.; Lopez, G.; Perez, J.; Chaloner, P. A.; Hitchcock, P. B. *Inorg. Chem.* **2003**, *42*, 3650–3661. (e) Crutchley, R. J.; Powell, J.; Faggiani, R.; Lock, C. J. L. *Inorg. Chim. Acta* **1977**, *24*, L15–L16. (f) Ozawa, F.; Son, T.; Ebina, S.; Osakada, K.; Yamamoto, A. *Organometallics* **1992**, *11*, 171–176. (g) Amatore, C.; Gamez, S.; Jutand, A.; Meyer, G.; Moreno-Manas, M.; Morral, L.; Pleixats, R. *Chem. - Eur. J.* **2000**, *6*, 3372–3376.

(12) Urry, W. H.; Kharasch, M. S. *J. Am. Chem. Soc.* **1944**, *66*, 1438–1440.

(13) (a) Seubold, F. H., Jr. *J. Am. Chem. Soc.* **1953**, *75*, 2532–2533. (b) Wilt, J. W.; Pawlikowski, W. W., Jr. *J. Org. Chem.* **1975**, *40*, 3641–3644. (c) Burton, A.; Ingold, K. U.; Walton, J. C. *J. Org. Chem.* **1996**, *61*, 3778–3782. (d) Weber, M.; Fischer, H. *J. Am. Chem. Soc.* **1999**, *121*, 7381–7388. (e) Chen, Z.-M.; Zhang, X.-M.; Tu, Y.-Q. *Chem. Soc. Rev.* **2015**, *44*, 5220–5245.

(14) (a) Heck, R.; Winstein, S. *J. Am. Chem. Soc.* **1957**, *79*, 3432–3438. (b) Saunders, W. H., Jr.; Paine, R. H. *J. Am. Chem. Soc.* **1961**, *83*, 882. (c) Shubin, V. G. *Top. Curr. Chem.* **1984**, *116/117*, 267–341.

(15) Campora, J.; Gutierrez-Puebla, E.; Lopez, J. A.; Monge, A.; Palma, P.; del Rio, D.; Carmona, E. *Angew. Chem., Int. Ed.* **2001**, *40*, 3641.

(16) Zhugralin, A. R.; Kobylanskii, I. J.; Chen, P. *Organometallics* **2015**, *34*, 1301–1306.

(17) O'Reilly, M. E.; Dutta, S.; Veige, A. S. *Chem. Rev.* **2016**, *116*, 8105–8145.

(18) (a) Langford, C. H.; Gray, H. B. *Ligand Substitution Processes*; Benjamin: New York, 1965. (b) Banerjee, P. *Coord. Chem. Rev.* **1999**, *190–192*, 19–28.

(19) (a) Sandstrom, J. *Dynamic NMR Spectroscopy*; Academic Press: London, 1982. (b) Nakamoto, K. *Infrared and Raman Spectra of Inorganic and Coordination Compounds*, 5th ed.; Wiley-Interscience: New York, 1997.

(20) (a) Seubert, K.; Bohme, D.; Koster, J.; Shen, W.-Z.; Freisinger, E.; Muller, J. Z. *Anorg. Allg. Chem.* **2012**, *638*, 1761–1767. (b) Nagy, Z.; Fabian, I.; Benyei, A.; Sovago, I. *J. Inorg. Biochem.* **2003**, *94*, 291–299. (c) Kim, S.; Kim, D.; Song, Y.; Lee, H.-J.; Lee, H. *Aust. J. Chem.* **2014**, *67*, 953–961. (d) Petersen, A. R.; White, A. J. P.; Britovsek, G. J. P. *Dalton Trans.* **2016**, *45*, 14520–14523. (e) McSkimming, A.; Diachenko, V.; London, R.; Olrich, K.; Onie, C. J.; Bhadbhade, M. M.; Bucknall, M. P.; Read, R. W.; Colbran, S. B. *Chem. - Eur. J.* **2014**, *20*, 11445–11456. (f) Mandapati, P.; Giesbrecht, P. K.; Davis, R. L.; Herbert, D. E. *Inorg. Chem.* **2017**, *56*, 3674–3685.

(21) Yang, L.; Powell, D. R.; Houser, R. P. *Dalton Trans.* **2007**, 955–964.

(22) (a) Lynch, J. E.; Eliel, E. L. *J. Am. Chem. Soc.* **1984**, *106*, 2943–2948. (b) Nave, S.; Sonawane, R. P.; Elford, T. G.; Aggarwal, V. K. *J. Am. Chem. Soc.* **2010**, *132*, 17096–17098. (c) Movahhed, S.; Westphal, J.; Dindaroglu, M.; Falk, A.; Schmalz, H.-G. *Chem. - Eur. J.* **2016**, *22*, 7381–7384. (d) Fernández-Mateos, A.; Madrazo, S. E.; Teijón, P. H.; González, R. R. *J. Org. Chem.* **2009**, *74*, 3913–3918. (e) Alacid, E.; Nájera, C. *Org. Lett.* **2008**, *10*, 5011–5014. (f) Terao, J.; Nakamura, M.; Kambe, N. *Chem. Commun.* **2009**, 6011–6013.

(23) (a) Thorshaug, K.; Fjeldahl, I.; Romming, C.; Tilset, M. *Dalton Trans.* **2003**, 4051–4056. (b) Aye, K.-T.; Vittal, J. J.; Puddephatt, R. J. *J. Chem. Soc., Dalton Trans.* **1993**, 1835–1839.

(24) (a) Smythe, N. A.; Grice, K. A.; Williams, B. S.; Goldberg, K. I. *Organometallics* **2009**, *28*, 277–288. (b) Desnoyer, A. N.; Love, J. A. *Chem. Soc. Rev.* **2017**, *46*, 197–238. (c) Sberegaeva, A. V.; Zavalij, P. Y.; Vedernikov, A. N. *J. Am. Chem. Soc.* **2016**, *138*, 1446–1455. (d) Pal, S.; Vedernikov, A. N. *Dalton Trans.* **2012**, *41*, 8116–8122. (e) Safa, M.; Jennings, M. C.; Puddephatt, R. J. *Organometallics* **2012**, *31*, 3539–3550. (f) Mitton, S. J.; McDonald, R.; Turculet, L. *Polyhedron* **2013**, *52*, 750–754.

(25) The structures of **6**, **O**, and **P** in the presence of aqueous hydrogen peroxide will certainly involve hydrogen bonding to solvent molecules, and the structures and relative energies shown in Figure 8 will consequently be modified. We do not claim that the 3-hydroxypropyl group plays a critical role in this reaction, and preliminary results indicate that the chemistry is similar with the corresponding ligand having a 3-methoxypropyl substituent.

(26) (a) Byers, P. K.; Canty, A. J.; Crespo, M.; Puddephatt, R. J.; Scott, J. D. *Organometallics* **1988**, *7*, 1363–1367. (b) Hyvl, J.; Roithova, J. *Org. Lett.* **2014**, *16*, 200–203. (d) Tang, F. Z.; Zhang, Y.; Rath, N. P.; Mirica, L. M. *Organometallics* **2012**, *31*, 6690–6696. (e) Xu, L.-M.; Li, B.-J.; Yang, Z.; Shi, Z.-J. *Chem. Soc. Rev.* **2010**, *39*, 712–733. (f) Racowski, J. M.; Dick, A. R.; Sanford, M. S. *J. Am. Chem. Soc.* **2009**, *131*, 10974–10983.

(27) (a) SAINT, version 2013.8; Bruker-AXS: Madison, WI, 2013. (b) SADABS, version 2012.1; Bruker-AXS: Madison, WI, 2012. (c) Sheldrick, G. M. *Acta Crystallogr., Sect. A: Found. Adv.* **2015**, *71*, 3. (d) Sheldrick, G. M. *Acta Crystallogr., Sect. C: Struct. Chem.* **2015**, *71*, 3.

(28) (a) Te Velde, G.; Bickelhaupt, F. M.; Baerends, E. J.; van Gisbergen, S.; Guerra, C. F.; Snijders, J. G.; Ziegler, T. *J. Comput. Chem.* **2001**, *22*, 931–967. (b) Becke, A. *Phys. Rev. A: At, Mol., Opt. Phys.* **1988**, *38*, 3098–3100.